

## Coordination of leaf structure and gas exchange along a height gradient in a tall conifer

D.R. WOODRUFF,<sup>1,2</sup> F.C. MEINZER,<sup>1</sup> B. LACHENBRUCH<sup>3</sup> and D.M. JOHNSON<sup>1</sup>

<sup>1</sup> USDA Forest Service, Forestry Sciences Laboratory, Corvallis, OR 97331, USA

<sup>2</sup> Corresponding author (david.woodruff@oregonstate.edu)

<sup>3</sup> Department of Wood Science and Engineering, Oregon State University, Corvallis, OR 97331, USA

Received June 6, 2008; accepted October 3, 2008

**Summary** The gravitational component of water potential and frictional resistance during transpiration lead to substantial reductions in leaf water potential ( $\Psi_l$ ) near the tops of tall trees, which can influence both leaf growth and physiology. We examined the relationships between morphological features and gas exchange in foliage collected near the tops of Douglas-fir (*Pseudotsuga menziesii* (Mirb.) Franco) trees of different height classes ranging from 5 to 55 m. This sampling allowed us to investigate the effects of tree height on leaf structural characteristics in the absence of potentially confounding factors such as irradiance, temperature, relative humidity and branch length. The use of cut foliage for measurement of intrinsic gas-exchange characteristics allowed identification of height-related trends without the immediate influences of path length and gravity. Stomatal density, needle length, needle width and needle area declined with increasing tree height by  $0.70 \text{ mm}^{-2} \text{ m}^{-1}$ ,  $0.20 \text{ mm m}^{-1}$ ,  $5.9 \times 10^{-3} \text{ mm m}^{-1}$  and  $0.012 \text{ mm}^2 \text{ m}^{-1}$ , respectively. Needle thickness and mesophyll thickness increased with tree height by  $4.8 \times 10^{-2} \text{ mm m}^{-1}$  and  $0.74 \text{ } \mu\text{m m}^{-1}$ , respectively. Mesophyll conductance ( $g_m$ ) and  $\text{CO}_2$  assimilation in ambient  $[\text{CO}_2]$  ( $A_{\text{amb}}$ ) decreased by  $1.1 \text{ mmol m}^{-2} \text{ s}^{-1} \text{ per m}$  and  $0.082 \text{ } \mu\text{mol m}^{-2} \text{ s}^{-1} \text{ per m}$  increase in height, respectively. Mean reductions in  $g_m$  and  $A_{\text{amb}}$  of foliage from 5 to 55 m were 47% and 42%, respectively. The observed trend in  $A_{\text{amb}}$  was associated with  $g_m$  and several leaf anatomic characteristics that are likely to be determined by the prevailing vertical tension gradient during foliar development. A linear increase in foliar  $\delta^{13}\text{C}$  values with height ( $0.042\text{‰ m}^{-1}$ ) implied that relative stomatal and mesophyll limitations of photosynthesis in intact shoots increased with height. These data suggest that increasing height leads to both fixed structural constraints on leaf gas exchange and dynamic constraints related to prevailing stomatal behavior.

**Keywords:** growth limitation, leaf anatomy, mesophyll conductance, photosynthesis, *Pseudotsuga menziesii*.

### Introduction

Several mechanisms have been studied as factors potentially responsible for reduced growth in trees as they age and increase in height, none of which are mutually exclusive. Proposed mechanisms include, but are not limited to, reduced leaf area as a result of reduced nutrient availability (Gower et al. 1996), genetics-related reductions in photosynthetic capacity induced by a limited capacity for repeated meristematic divisions (Haffner et al. 1991), reduced photosynthesis in response to increased hydraulic resistance with increased tree height (Mencuccini and Grace 1996, Ryan and Yoder 1997, McDowell et al. 2002), reduced foliar expansion due to lower turgor pressure (Koch et al. 2004, Woodruff et al. 2004), and reduced leaf hydraulic efficiency as a result of height-related restrictions on leaf expansion (Woodruff et al. 2008). Available evidence suggests that it is the size (height) as opposed to the age that is primarily responsible for ontogenetic patterns in growth (Koch et al. 2004, Woodruff et al. 2004, Bond et al. 2007, Mencuccini et al. 2007). Studies on how height affects gas exchange in trees have not yet parsed out the extrinsic effects of path length and gravity from the intrinsic effects of height-related trends in foliar structural characteristics on gas exchange.

Leaf structural characteristics can influence gas exchange through their effects on the efficiency or capacity of processes such as light absorption, carbon fixation and control of water loss. Leaf structural characteristics that influence gas exchange can vary in response to changes or gradients in environmental conditions (reviewed in Abrams 1994, Gutschick 1999), in response to increased age or height (Apple et al. 2002, England and Attiwill 2006) and in response to vertical water potential gradients (Koch et al. 2004, Woodruff et al. 2004, 2008). Mesophyll cells comprise the bulk of foliar tissue and represent the site of two types of resistance that can influence  $\text{CO}_2$  assimilation ( $A$ ): resistance to the transport of water from leaf veins and xylem conduits to stomata, and resistance to the movement of

CO<sub>2</sub> from the intercellular air spaces to the sites of carboxylation inside the chloroplasts.

There are two predominant resistances to the diffusion of CO<sub>2</sub> as it moves from the atmosphere to the sites of carboxylation inside the leaf. Stomatal resistance occurs as CO<sub>2</sub> diffuses through the stomata and into the sub-stomatal cavities. The less-studied type of foliar resistance to CO<sub>2</sub> uptake is mesophyll resistance ( $r_m$ , the inverse of mesophyll conductance,  $g_m$ ) that involves the resistance to CO<sub>2</sub> diffusion through the mesophyll cell walls and membranes, and through the liquid phase inside the mesophyll cells. At the mesophyll cell surface, CO<sub>2</sub> enters the liquid phase and moves through the cell wall and through the chloroplast membrane to the site of carboxylation. Mesophyll resistance to CO<sub>2</sub> transfer can account for a substantial proportion of the total resistance to CO<sub>2</sub> transfer. Recent research has begun to reveal the importance of internal leaf conductance for gas exchange. Niinemets (1997) found a direct correlation between  $g_m$  and  $A$  in *Picea abies* (L.) H. Karst, both of which decreased with increasing tree age, and speculated that reductions in  $g_m$  may be a factor in size-related reductions in  $A$  for *Picea abies* and *Pinus sylvestris* L. (Niinemets 2002). Across a range of 50 species, internal leaf resistance accounted for about 40% of the decrease in CO<sub>2</sub> concentration ([CO<sub>2</sub>]) between the atmosphere and sites of carboxylation (Syvertsen et al. 1995, Hanba et al. 1999, Warren 2008 and references therein, Flexas et al. 2008). The determinants of internal leaf conductance are not yet fully understood, but are likely to include a combination of leaf anatomic and biochemical factors (Warren 2008). Leaf mesophyll structural characteristics that could affect the movement of either water or CO<sub>2</sub> are thus likely to have an effect on  $A$ .

Douglas-fir (*Pseudotsuga menziesii* (Mirb.) Franco) is one of the world's tallest tree species (Carder 1995) and can attain a height of > 100 m. The aim of this study was to determine the extent to which height imposes developmental constraints on Douglas-fir foliage that lead to intrinsic limitations for gas exchange. Two questions were investigated: (1) What effect does tree height have on the structural characteristics of Douglas-fir foliage? (2) Are there limitations on gas exchange associated with intrinsic leaf structural characteristics that can be attributed to path length and gravity during the time of foliar development? We hypothesized that height-related trends in leaf structure impose constraints on leaf gas exchange that are independent of the direct effects of vertical gradients in xylem tension on stomatal and photosynthetic physiology.

## Materials and methods

### Field site and sampling

Four stands, each containing Douglas-fir trees of a different height class, were located within 3.1 km of each other in the Wind River Basin of southwestern Washington, USA.

Access to tree tops in the 55-m sampling height class was facilitated by a 75-m-tall construction tower crane at the Wind River Canopy Crane Research Facility (WRCCRF). Periodic dieback of the tops of some of the trees within the WRCCRF stand suggested that these trees were close to their maximum height for this site. Tree tops in the two intermediate height classes were accessed by non-spur climbing and foliage from the lowest height class was accessed with a pole pruner. We collected 30–50-cm-long branch samples within 1–5 m of the tops of the trees at mean sampling heights of 5.0, 18.3, 33.5 and 55.0 m. All samples were obtained from fully sun-exposed locations during the summer and fall of 2007. Branches were collected from trees early in the morning before significant transpirational water loss and were placed in plastic bags with moist paper towels and stored in the dark at 5 °C.

The Pacific maritime climate of the region is characterized by wet winters and dry summers. Mean annual precipitation in the region is about 2.2 m, much of which falls as snow, with a dry season from June to September. Mean annual temperature is 8.7 °C with a mean of 0 °C in January and 17.5 °C in July. The soils are well drained and of volcanic origin (Shaw et al. 2004). Low precipitation between June and September (~ 119 mm) typically leads to drought conditions in the upper portion of the soil profile. However, soil water remains accessible to Douglas-fir roots at depths greater than about 1 m throughout the summer dry period (Warren et al. 2005, Meinzer et al. 2007).

### Leaf structural characteristics

We measured stomatal density ( $D_s$ ), length ( $L_n$ ), width ( $W_n$ ), thickness ( $T_n$ ), area (LA) and mesophyll thickness ( $T_m$ ) of Douglas-fir needles. All needles were sampled exclusively from fully sun-exposed branches near the tops of trees of different height classes to rule out the potentially confounding influence of factors such as irradiance, relative humidity, and branch length upon height-related trends in leaf structural characteristics. Needle width, length and thickness were measured with digital calipers. Three needles were measured from  $n = 3$  branches per tree. Leaf areas were measured on 10 needles per branch, on  $n = 3$  branches per tree and three trees per height class. One-sided leaf areas were obtained using a scanner and ImageJ Version 1.27 image analysis software (Abramoff et al. 2004).

Mesophyll thickness ( $T_m$ ), which was used as a proxy for the distance necessary for water to move through mesophyll tissue inside the leaf, was estimated as the distance between the outside of the endodermis and the nearest inside edge of the leaf epidermis. Cross sections of needles were made by hand sectioning fresh tissue and mounting them on slides. Needle cross sections were analyzed for  $T_m$  with an image analysis system consisting of a compound microscope and a video camera. Three needles were analyzed from each of three branches, for a total of nine measurements per tree. Images were obtained using 10× objectives and a total

magnification of 100×. Data were pooled per tree and subjected to regression analysis. Stomatal density was measured with a dissecting microscope and a linear scale in millimeter increments. Stomata were counted over a 1-mm length near the center of the needles. Number of stomata per millimeter of needle length was divided by needle width to generate number of stomata per mm<sup>2</sup> leaf area. Three needles were counted from each of  $n = 4\text{--}5$  branches per tree.

#### *Gas exchange and carbon isotope ratios*

We evaluated several parameters related to  $A$  using photosynthetic CO<sub>2</sub> response curves, including  $A$  at ambient [CO<sub>2</sub>] ( $A_{\text{amb}}$ ), maximum  $A$  ( $A_{\text{max}}$ ), maximum carboxylation rate allowed by ribulose 1,5-bisphosphate carboxylase/oxygenase (Rubisco) ( $V_{\text{cmax}}$ ), rate of photosynthetic electron transport ( $J$ ), and mesophyll conductance ( $g_m$ ). These parameters were measured on branches sampled from the tops of trees of different height classes. We conducted measurements in the laboratory on detached shoots that had their bases immersed in water to eliminate the immediate effects of path length and gravity on gas exchange, thereby enabling us to isolate the influence of any height-related trends in foliar structure on the various gas exchange parameters. Before starting the gas-exchange measurement, we detached shoots of about 15–20 cm in length from the larger branch samples, taking care to submerge the shoot bases in degassed water as the cut was made. Our previous work on attached and detached Douglas-fir foliage showed that Douglas-fir shoots retain the same gas-exchange characteristics for about 4 days after detachment. In this study, mean  $A_{\text{max}}$  for samples taken at a tree height of 55 m at 0, 1 and 2 days following excision were 16.5, 14.6 and 19.7  $\mu\text{mol m}^{-2} \text{s}^{-1}$ , respectively ( $P = 0.25$  for regression analysis of  $A_{\text{max}}$  versus days since excision). This lack of a decrease in  $A_{\text{max}}$  suggests that the foliage was still fully active physiologically throughout the period of branch detachment while measurements were conducted.

Gas exchange was measured with a portable photosynthesis system equipped with a red or blue LED source and CO<sub>2</sub> injector (LI-6400, Li-Cor, Lincoln, NE). The instrument was zeroed and the chemicals were replaced prior to use each day. For determination of the dependence of CO<sub>2</sub> assimilation ( $A$ ) on intercellular CO<sub>2</sub> concentration ( $A\text{--}C_i$  curves), photosynthetic photon flux was held at 1200  $\mu\text{mol m}^{-2} \text{s}^{-1}$ , vapor pressure deficit at 1.0 kPa and leaf temperature at 25 °C. The cuvette [CO<sub>2</sub>] was initially set near ambient, progressively lowered to 50 ppm, increased directly to ambient, and then progressively increased. The ambient [CO<sub>2</sub>] were set at the following values and order: 400, 300, 200, 100, 50, 400, 400, 600, 800, 1000, 1200, and then increased at 200-ppm intervals until no further response of  $A$  was observed. Leaves were allowed to equilibrate for at least 2 min following the increase in [CO<sub>2</sub>]. Branch samples were measured within 1–3 days of excision. Gas-exchange measurements were

made on  $n = 2$  branches per tree, and on three trees per height class.

The  $A\text{--}C_i$  curves were used to estimate  $g_m$ ,  $V_{\text{cmax}}$  and  $J$  using a utility developed by Sharkey et al. (2007) based on an alternative  $A\text{--}C_i$  curve fitting method (Ethier and Livingston 2004) that accounts for CO<sub>2</sub> transfer conductance through a non-rectangular hyperbola version of the model of Farquhar et al. (1980). In this model, the biochemical reactions of photosynthesis are considered to be limited either by the properties of Rubisco, the regeneration of the substrate ribulose bisphosphate (RuBP), or by triose-phosphate use limitation. When  $A$  is Rubisco-limited, the response of  $A$  to [CO<sub>2</sub>] can be described:

$$A = V_{\text{cmax}}[C_C - \Gamma^*/C_C + K_C(1 + O/K_O)] - R_d, \quad (1)$$

where  $C_C$  and  $O$  are the partial pressures of CO<sub>2</sub> and oxygen, respectively, at the sites of carboxylation,  $\Gamma^*$  is [CO<sub>2</sub>] at which oxygenation proceeds at twice the rate of carboxylation causing photosynthetic uptake of CO<sub>2</sub> to be exactly compensated by photorespiratory CO<sub>2</sub> release,  $K_C$  is the Michaelis constant of Rubisco for CO<sub>2</sub>,  $K_O$  is the inhibition constant of Rubisco for oxygen, and  $R_d$  is day respiration. When  $A$  is limited by RuBP regeneration:

$$A = J[C_C - \Gamma^*/4C_C + 8\Gamma^*] - R_d, \quad (2)$$

where  $J$  is rate of electron transport. In the  $A\text{--}C_i$  utility used to analyze photosynthesis,  $C_C$  is replaced with ( $C_i\text{--}A/g_m$ ) and  $g_m$  is estimated from the observed data by nonlinear curve fitting and minimizing the sum of squared model deviations. Ideally a second method for determining  $g_m$ , such as combined fluorescence and gas exchange, would be employed to verify the results from the curve analyses. However, the combined fluorescence and gas-exchange method is ill-suited for measurements of conifers (Ülo Niinemets, personal communication), and the previous research has shown a high correlation between the Ethier and Livingston (2004) method and the combined fluorescence and gas-exchange method (Niinemets et al. 2005). The accuracy of estimating  $g_m$  with the Sharkey utility can be enhanced by maximizing the number of values in the curvature region of the  $A\text{--}C_i$  relationship (Ethier and Livingston 2004). The  $A\text{--}C_i$  curves in this study were created and analyzed in a manner so as to minimize the sum of squares error in the models and maximize the number of values within the curvature region. The mean number of values in the curvature region of the curves was 6.8 (SE = 0.31), 5.8 (SE = 0.48), 8.8 (SE = 0.95) and 5.6 (SE = 0.37) for the foliage sampled from the trees at mean sampling heights of 5.0, 18.3, 33.5 and 55.0 m, respectively.

We determined the mean value of  $C_i$  at standard ambient [CO<sub>2</sub>] (385 ppm) for all  $A\text{--}C_i$  curves to characterize photosynthetic parameters at standard ambient [CO<sub>2</sub>]. The mean leaf internal [CO<sub>2</sub>] at 385 ppm sample [CO<sub>2</sub>] was 235 ppm

Table 1. Characteristics of foliage sampled within 1–5 m of the tops of *P. menziesii* trees at mean sampling heights of 5.0, 18.3, 34.5 and 55.0 m (mean values with SE in parentheses). Internal [CO<sub>2</sub>] at ambient [CO<sub>2</sub>] ( $C_i$  at  $C_a = 385$  ppm).

Height (m)	$N_A$ (g m <sup>-2</sup> )	$A_{max}$ (μmol m <sup>-2</sup> s <sup>-1</sup> )	$A/g_s$ (μmol mol <sup>-1</sup> )	$C_i$ at $C_a = 385$ ppm (ppm)	$V_{cmax}$ (μmol m <sup>-2</sup> s <sup>-1</sup> )	$g_m$ (mmol m <sup>-2</sup> s <sup>-1</sup> )	$J$ (μmol m <sup>-2</sup> s <sup>-1</sup> )
5 (0)	1.9 (0.13)	21 (0.3)	94 (10)	224 (13)	95 (0.6)	106 (3.4)	104 (1.3)
18.3 (0.3)	1.8 (0.07)	20 (0.5)	96 (10)	219 (7)	105 (1.8)	84 (3.6)	112 (8.3)
33.5 (1.3)	1.8 (0.11)	21 (1.3)	72 (12)	248 (13)	139 (3.8)	43 (2.9)	134 (6.4)
55 (1.1)	1.5 (0.08)	17 (0.4)	62 (8)	252 (12)	77 (10)	56 (3.9)	104 (4.8)

(SE = 6.25) (Table 1). Carbon dioxide assimilation at ambient [CO<sub>2</sub>] ( $A_{amb}$ ) was determined by first establishing a mean  $C_i$  value for ambient [CO<sub>2</sub>] (385 ppm) and then determining  $A$  at that  $C_i$  value for each  $A$ – $C_i$  curve. Instantaneous water use efficiency ( $A/g_s$ ) was determined by dividing  $A_{amb}$  by stomatal conductance ( $g_s$ ) at  $C_i = 235$  ppm.

Stable carbon isotope analysis was conducted on leaf tissue to determine integrated intrinsic water-use efficiency. Foliage on which gas exchange was measured plus foliage from one additional branch per tree was collected, dried and ground, and analyzed for δ<sup>13</sup>C and nitrogen concentration ([N]) with a Carla Erba 1110 elemental analyzer coupled to a Thermo Finnigan Delta S isotope ratio mass spectrometer through an open split interface (Stable Isotope Ratio Facility for Environmental Research, University of Utah). Integrated water-use efficiency ( $A/g_{s-integrated}$ ) was obtained as (Farquhar et al. 1982):

$$A/g_{s-integrated} = (C_a - C_i)/1.6. \quad (3)$$

An analysis of the vertical trend in integrated, in situ photosynthesis ( $A_{integrated}$ ) was performed by calculating  $A$  from needle δ<sup>13</sup>C values. We determined discrimination ( $\Delta$ ) against <sup>13</sup>C in leaf tissue as (Farquhar et al. 1982):

$$\Delta = \delta_{source} - \delta_{product}/1 + (\delta_{source}/1000), \quad (4)$$

where  $\delta_{source} = \delta^{13}C$  for atmospheric CO<sub>2</sub> (–8‰),  $\delta_{product} = \delta$  and <sup>13</sup>C for leaf tissue. We then used Eq. (5), also from Farquhar et al. (1982), to obtain  $C_i$  at standard atmospheric [CO<sub>2</sub>] ( $C_a = 385$  ppm):

$$\Delta = a + (b - a)C_i/C_a, \quad (5)$$

where  $a$  = discrimination against <sup>13</sup>C during diffusion (4.4‰) and  $b$  = discrimination against <sup>13</sup>C during the carboxylation reaction (27.0‰). By rearranging Eq. (5) we were able to solve for  $C_i$ :

$$C_i = C_a(\Delta - a/b - a). \quad (6)$$

The intercellular [CO<sub>2</sub>] is typically used in place of  $C_C$  in plant ecophysiological research because  $C_C$  cannot be estimated from gas-exchange measurements. Values of δ<sup>13</sup>C reflect  $C_C$ , not  $C_i$ , and this analysis can lead to overestimates of  $A/g_{s-integrated}$ . The degree to which  $C_i$  varies from  $C_C$  is dependent on  $r_m$ , with higher values of  $r_m$  corresponding to greater overestimation of  $A/g_{s-integrated}$ .

We used the three-parameter exponential equation  $y = y_0 + a(1 - e^{-bx})$  describing the dependence of  $A$  on  $C_i$  obtained from gas-exchange measurements in the laboratory to estimate  $A$  from the  $C_i$  values obtained from foliar δ<sup>13</sup>C. This methodology assumes that the non-stomatal, photosynthetic characteristics of the foliage are not substantially influenced by detachment. The value of  $g_{s-integrated}$  is determined from estimates of  $A/g_{s-integrated}$  and  $A_{integrated}$ . Stable isotope analyses were conducted on  $n = 3$  branches per tree, and on three trees per height class.

Maximum leaf hydraulic conductance ( $K_{leaf-max}$ ) was measured by methods adapted from Brodrigg and Holbrook (2003) as described by Woodruff et al. (2008). The method involves use of Eq. (7) which is derived from the relationship between rehydrating a leaf and recharging a capacitor:

$$K_{leaf} = C \ln(\Psi_o \Psi_f)t, \quad (7)$$

where  $K_{leaf}$  = leaf hydraulic conductance,  $C$  = capacitance,  $\Psi_o$  = leaf water potential before rehydration,  $\Psi_f$  = leaf water potential after rehydration, and  $t$  = duration of dehydration. We determined  $C$  on an individual tree basis from the slope of the relationship between relative water content and leaf water potential ( $\Psi_l$ ) obtained from pressure–volume curves.

## Results

### Leaf structural characteristics

There were height-related trends in the examined leaf morphological characteristics (Figure 1). A 0.2 mm decline in needle length per meter increase in height was the single most significant trend in needle morphology ( $P < 0.0001$ ). One-sided needle area showed the next most significant height-related trend, declining by 0.21 mm<sup>2</sup> for every meter increase in height ( $P = 0.0004$ ). Needle width declined with increasing height by  $5.9 \times 10^{-3}$  mm m<sup>-1</sup> ( $P = 0.0025$ ), and needle thickness increased with height by  $8.9 \times 10^{-4}$  mm m<sup>-1</sup> ( $P = 0.0011$ ). Stomatal density showed a significant linear decline with increasing height of  $-0.7$  stomata mm<sup>-2</sup> m<sup>-1</sup> ( $P = 0.0032$ ), but a three-parameter exponential decay function ( $y = y_0 + ae^{-bx}$ ) yielded an improved regression fit with  $r^2 = 0.77$  (data not shown) suggesting a possible limit to the reduction in

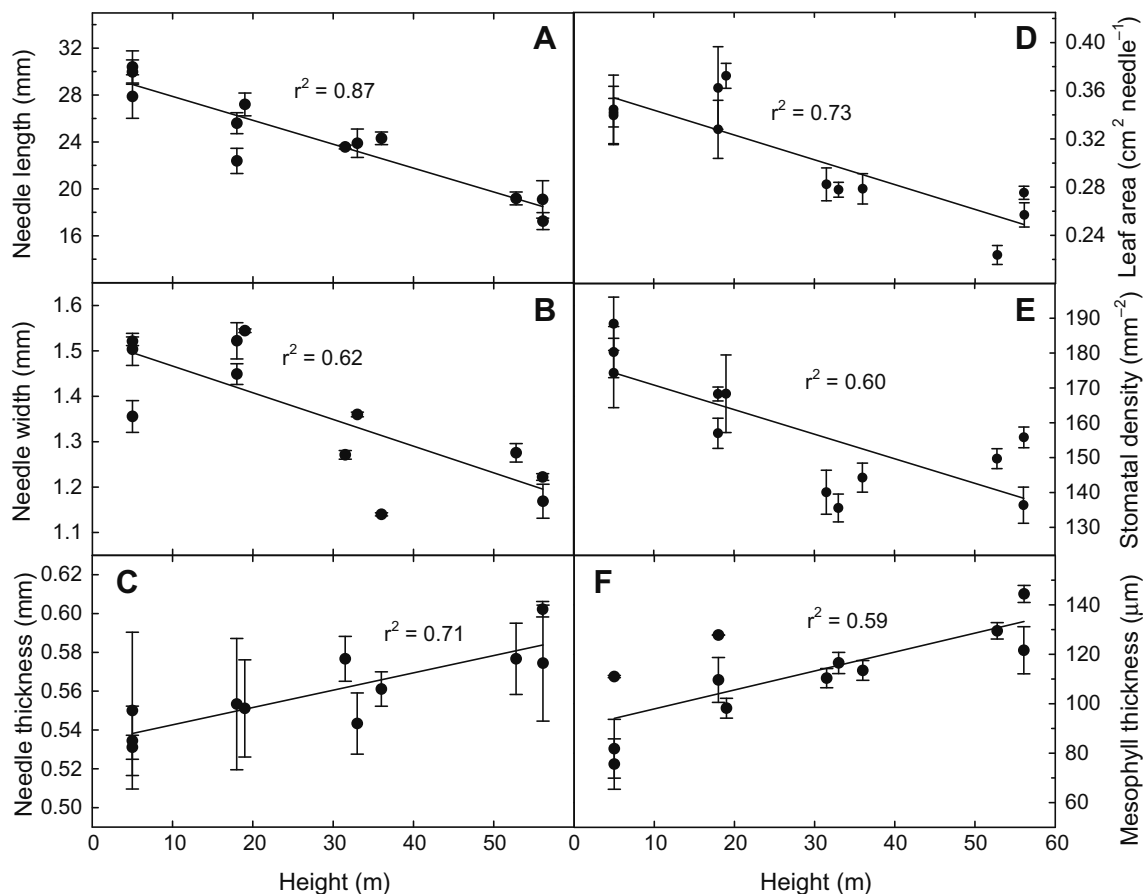


Figure 1. Leaf anatomic and structural characteristics in relation to tree height for foliage samples obtained within 1–5 m of the tops of *P. menziesii* trees at mean sampling heights of 5.0, 18.3, 34.5 and 55.0 m. Needle length (A), needle width (B), needle thickness (C), leaf area per needle (D), stomatal density (E) and mesophyll thickness (F). Bars denote  $\pm$  SE,  $n = 3$  branches per tree for (A), (B), (C), (D) and (F);  $n = 4$  branches for (E).

stomatal density with increased height. Mesophyll thickness showed a significant increase with increasing height of  $0.74 \mu\text{m m}^{-1}$  ( $P = 0.0036$ ).

#### Gas exchange

Gas-exchange measurements showed that, in the initial portion of the  $A-C_i$  curves where  $A$  is heavily influenced by  $g_m$ ,  $A$  declined with increasing height (Figure 2). Mean ( $\pm$  SE)  $A_{\text{amb}}$  at 55 m was  $5.49 \pm 0.41 \mu\text{mol m}^{-2} \text{s}^{-1}$  and mean  $A_{\text{amb}}$  at 5 m was  $9.52 \pm 0.42 \mu\text{mol m}^{-2} \text{s}^{-1}$ , representing a 42% reduction in assimilation at ambient  $[\text{CO}_2]$  over a 50-m increase in height (Figures 2 and 3). There were significant linear reductions in both  $A_{\text{amb}}$  and  $g_m$  with increasing height ( $r^2 = 0.72$ ,  $P = 0.00051$ ;  $r^2 = 0.60$ ,  $P = 0.0032$ , respectively, data not shown). A three-parameter exponential decay function ( $y = y_0 + ae^{-bx}$ ) yielded improved regression fits with  $r^2 = 0.83$  and  $0.77$  for  $A_{\text{amb}}$  and  $g_m$  plotted against height, respectively (Figure 3). Plotting  $A_{\text{amb}}$  against  $g_m$  revealed a more significant relationship than either variable plotted against height ( $r^2 = 0.92$ ,  $P < 0.0001$ ), consistent with  $g_m$  as an important determi-

nant of  $A$  under non-saturating  $[\text{CO}_2]$  (Figure 3, inset). The correlation between  $A_{\text{max}}$  and height was also significant ( $r^2 = 0.45$ ,  $P = 0.017$ ; Table 1) although substantially less than the correlation between height and  $A_{\text{amb}}$ . Neither  $V_{\text{cmax}}$  nor  $J$  was significantly correlated with height ( $r^2 = 0.04$ ,  $P = 0.54$ ;  $r^2 = 0.005$ ,  $P = 0.83$ , respectively, Table 1). The correlation of nitrogen per unit leaf area ( $N_A$ ) with height was nearly significant ( $r^2 = 0.32$ ,  $P = 0.056$ ; Table 1). Foliar  $\delta_{13}\text{C}$  increased significantly with height by  $0.042\text{‰ m}^{-1}$  ( $P = 0.0002$ , data not shown). Integrated water-use efficiency increased significantly with height ( $P = 0.00019$ ) by  $0.45 \mu\text{mol mol}^{-1}$  for every 1 m increase in height (Figure 4A). In contrast to  $A/g_s$ -integrated, there was a slight but significant ( $P = 0.011$ ) decline in  $A/g_s$  with increasing height (Figure 4B). Mesophyll thickness was negatively correlated with both  $K_{\text{leaf-max}}$  ( $P = 0.00008$ ; Figure 5A) and  $A_{\text{max}}$  ( $P = 0.02$ ; Figure 5B). Both  $A_{\text{max}}$  and  $K_{\text{leaf-max}}$  were positively correlated with each other ( $P = 0.02$ , data not shown). Because  $A_{\text{integrated}}$  was estimated from foliar  $\delta_{13}\text{C}$ , it reflects the photosynthetic history of the foliage when the shoot was still attached to the tree. There was a linear decline in  $A_{\text{integrated}}$

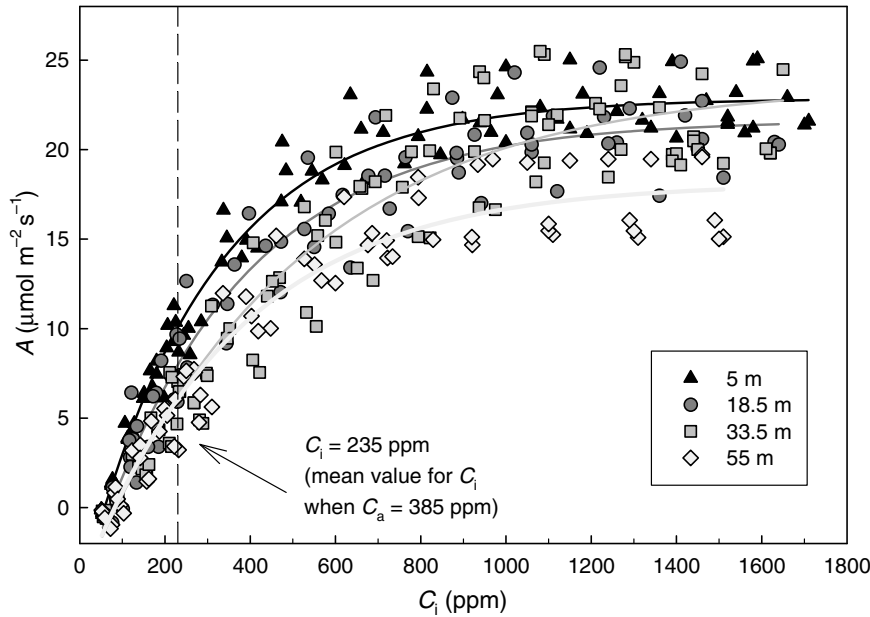


Figure 2. CO<sub>2</sub> assimilation rate ( $A$ ) versus intercellular CO<sub>2</sub> concentration ( $A$ - $C_i$  curves) for foliage sampled within 1–5 m of the tops of *P. menziesii* trees at mean sampling heights of 5.0, 18.3, 34.5 and 55.0 m. The vertical dashed line represents 235 ppm, the mean value for  $C_i$  at standard ambient [CO<sub>2</sub>] (385 ppm).

with increasing height ( $r^2 = 0.89$ ,  $P < 0.0001$ ), but the decline was steeper than that of  $A_{\text{amb}}$  with increasing height. A three-parameter exponential decay function yielded an improved regression fit with  $r^2 = 0.99$  for the dependence of  $A_{\text{integrated}}$  on height (Figure 6A). Mean integrated  $g_s$  ( $g_{s\text{-integrated}}$ ) was also negatively correlated with height ( $P = 0.0002$ ). A three-parameter exponential decay function yielded a regression fit with  $r^2 = 0.98$  (Figure 6B).

## Discussion

We were able to isolate gravity and path length as causal factors for trends in gas exchange by collecting our samples exclusively from the tops of Douglas-fir trees of different heights, within a localized geographic area, thereby eliminating appreciable differences in irradiance, humidity, temperature and branch length as confounding variables in the development of foliar characteristics that could influence gas exchange. These size-related trends in gas exchange of Douglas-fir can thus be attributed to intrinsic properties of the shoot that arise during tissue development.

### Leaf structural characteristics

Leaf structural characteristics can strongly affect processes involved in gas exchange such as light absorption, carbon fixation and water loss. Needle length, width and area each showed significant negative trends with increasing tree height, supporting earlier observations of reduced leaf expansion along height gradients within the crowns of individual Douglas-fir trees (Woodruff et al. 2004, Meinzer et al. 2007). Although one might assume that smaller leaves have higher stomatal density because of the tighter packing of stomata among the less expanded epidermal cells as has

often been reported in sun versus shade leaves (Givnish 1988, Osborn and Taylor 1990), we found a 19% reduction in mean stomatal density from the lowest to the tallest height class studied. Previous work has shown that cell division as well as expansion are sensitive to turgor pressure (Boyer 1968, Kirkham et al. 1972, Hsiao et al. 1976, Gould and Measures 1977), which could have implications for the mechanisms that control the differentiation of epidermal cells to stomata. Beerling and Chaloner (1993) found a reduction in stomatal density in *Quercus* with increased temperature, and suggested that the observed response was a possible adaptation to reduce water loss. Although reduced stomatal density will tend to limit capacity for  $A$ , particularly in leaves of higher density in which lateral movement of CO<sub>2</sub> through internal air spaces is limited (Parkhurst 1986), its primary consequence may be to reduce water loss, particularly in cases in which stomata do not completely close (Caird et al. 2007).

### Hydraulic resistance

The leaf mesophyll also presents a site of resistance to the transport of water from xylem conduits to the stomata. Water moves out of the leaf xylem and then through bundle sheath and mesophyll cells before evaporating in the intercellular air spaces. The resistance to water flow through living mesophyll tissue is substantially greater than through nonliving vessels and tracheids (Boyer et al. 1985), and thus mesophyll hydraulic resistance may represent a substantial limitation for gas exchange. Aasamaa et al. (2001) had found that the area of mesophyll and epidermal cells per unit length of leaf cross section was strongly and positively correlated with shoot hydraulic conductance across a range of deciduous trees. Brodribb et al. (2007) had found that across 43 species,  $A_{\text{max}}$  was correlated with the distance

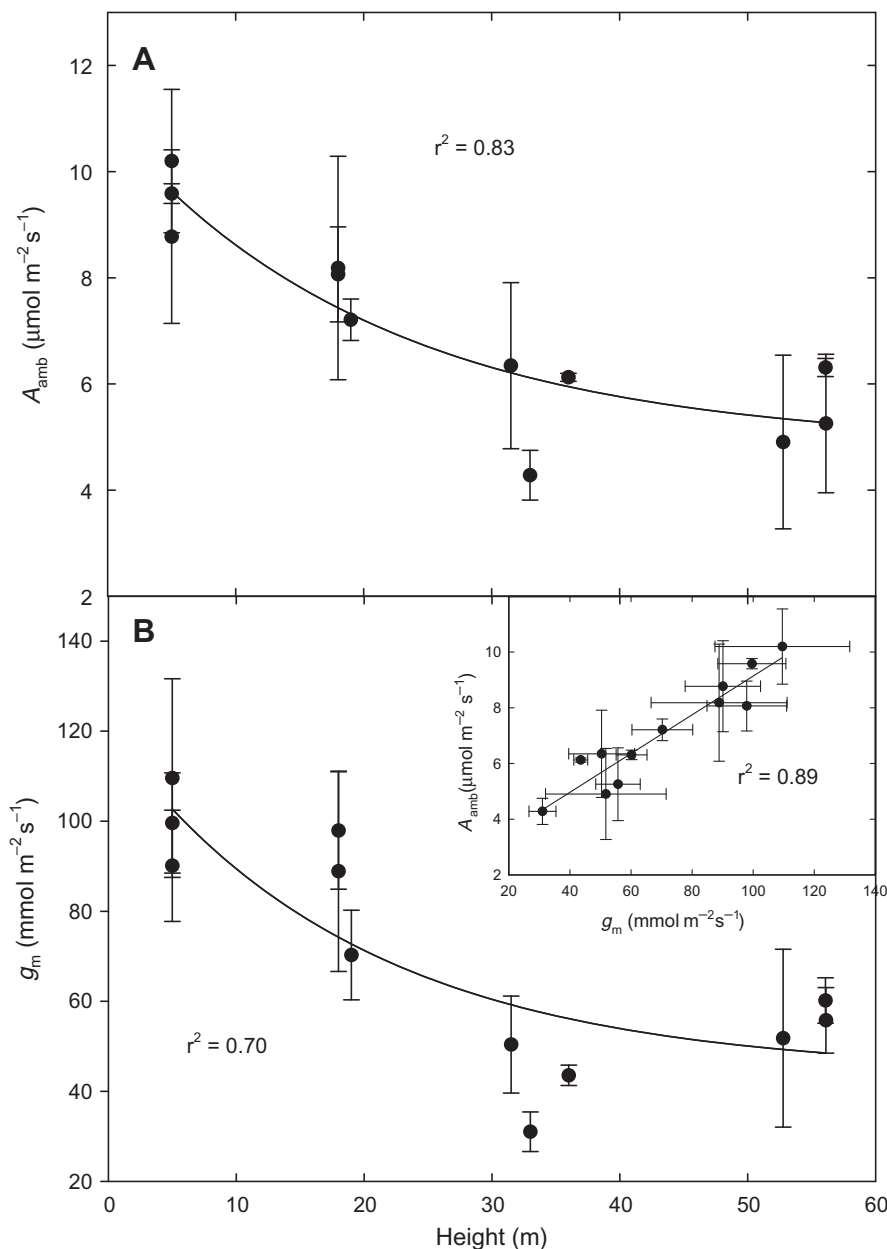


Figure 3. CO<sub>2</sub> assimilation rate at an intercellular CO<sub>2</sub> concentration of 235 ppm ( $A_{\text{amb}}$ ) versus height (A) and mesophyll conductance ( $g_m$ ) versus height (B) in *P. menziesii*. Inset shows  $A_{\text{amb}}$  versus  $g_m$ . Bars denote  $\pm$ SE,  $n = 2$  branches.

between veins and leaf surface and with  $K_{\text{leaf}}$ . They concluded that the relationship between vein location and photosynthetic rate was determined by the conductance of the leaf mesophyll to water flow. In our study, the highly significant correlation between  $T_m$  and  $K_{\text{leaf-max}}$  (Figure 5A) suggests that leaf structural characteristics that influence  $r_m$  can have a substantial influence on leaf hydraulic architecture, and subsequently photosynthesis.

#### Resistance to transfer of CO<sub>2</sub>

We found that the ratio of  $g_m$  from detached shoots to  $g_{s\text{-integrated}}$  estimated from foliar  $\delta_{13}\text{C}$  ranged from 0.47 to 0.71. Peña-Rojas et al. (2005) had found  $g_m$  in *Quercus* to be equal to about one-half of  $g_s$ . DeLucia et al. (2003)

had found  $g_m/g_s$  to be between 0.6 and 1.1 in conifers and between 1.0 and 4.2 in angiosperms, and in a survey of 50 species Warren (2008) had found  $g_m/g_s$  to be 1.3 in conifers and between 0.52 and 1.5 in angiosperms. We found a 47% reduction in mean  $g_m$  along a 50-m height gradient (Figure 3B), which was strongly correlated with variation in  $A_{\text{amb}}$  among height classes (Figure 3, inset). Mesophyll conductance is considered to be a key determinant of  $A$  at low values of  $C_i$  and thus the initial slope of  $A-C_i$  curves (Farquhar et al. 1980). Consistent with this relationship, the most pronounced differences in  $A$  between height classes were observed under non-saturated [CO<sub>2</sub>] ( $A_{\text{amb}}$ ; Figures 2 and 3), whereas the trend in  $A_{\text{max}}$  with increasing height was much less pronounced (Table 1). Given the importance of  $g_m$  as a determinant of  $A$  under

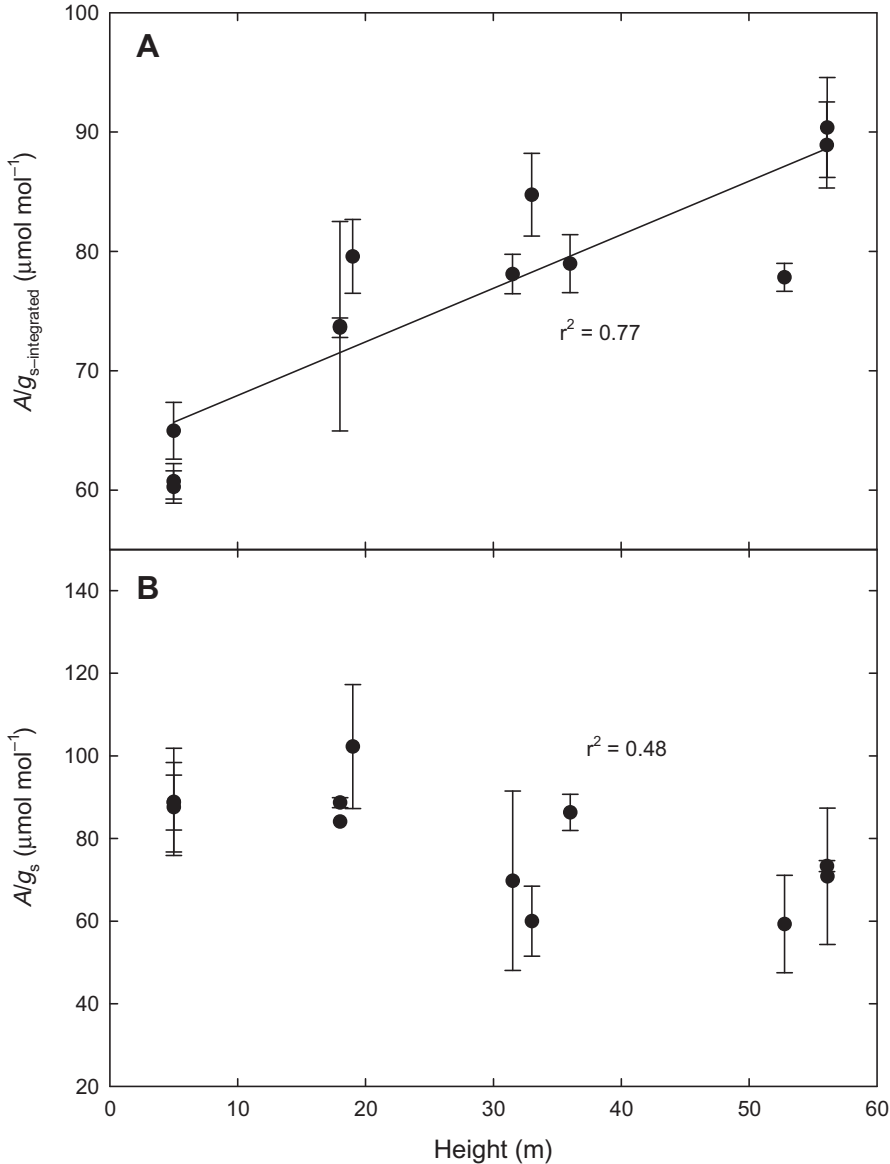


Figure 4. Integrated water-use efficiency ( $A/g_{s-integrated}$ ) versus height (A) and instantaneous water-use efficiency ( $A/g_s$ ) versus height (B) in *P. menziesii*. Bars denote  $\pm$ SE,  $n = 3$  branches for (A) and  $n = 2$  branches for (B).

non-saturating  $[CO_2]$ , the greater height-related decline in  $A_{amb}$  relative to that of  $A_{max}$  provides further evidence of  $g_m$  as a critical factor in the observed decline in  $A_{amb}$  with increasing height in Douglas-fir.

Water stress has been shown to lead to reductions in  $g_m$ , even in cases where the water stress is only moderate (O'Toole et al. 1976, Loreto et al. 1997, Peña-Rojas et al. 2005). A proposed mechanism for the water-stress-induced depression of  $g_m$  is through reduced leaf turgor and its influence on mesophyll surface area. The height-related decline in  $g_m$  in our study is thus likely to be associated with the effects of gravitational and transpirational xylem tension gradients on  $\Psi_l$  (Bauerle et al. 1999) and turgor during leaf expansion (Woodruff et al. 2004). Warren et al. (2004) had used simultaneous gas-exchange and isotopic measurements to determine  $g_m$  for Douglas-fir seedlings under different hydration regimes and found 73% higher  $g_m$  in well-watered Douglas-fir seedlings than in water-stressed

seedlings (0.076 and 0.044 mol m<sup>-2</sup> s<sup>-1</sup>, respectively). In the first study to report  $g_m$  in a conifer, Warren et al. (2003) had found that the mean  $g_m$  was 0.16 mol m<sup>-2</sup> s<sup>-1</sup> in the lower canopy (17–20 whorls down from the top) and 0.20 mol m<sup>-2</sup> s<sup>-1</sup> in the upper canopy (4–8 whorls down from the top) within the same 34-m-tall Douglas-fir tree. Their observed height-related increase in  $g_m$  suggests that light exposure within a tree crown may mask intrinsic height-related trends in  $g_m$ .

#### Nitrogen- and water-use efficiency

Nitrogen concentration per unit leaf area ( $N_A$ ) was 17% lower at 55 than at 5 m, and the correlation between height and  $N_A$  was nearly significant ( $P = 0.056$ ). The correlation between  $A_{max}$  and  $N_A$ , however, was more significant ( $P = 0.043$ ). The correlations of  $N_A$  with both  $A_{max}$  and  $A_{amb}$  ( $P = 0.052$ ); and  $g_m$  with both  $A_{max}$  ( $P = 0.3$ ) and

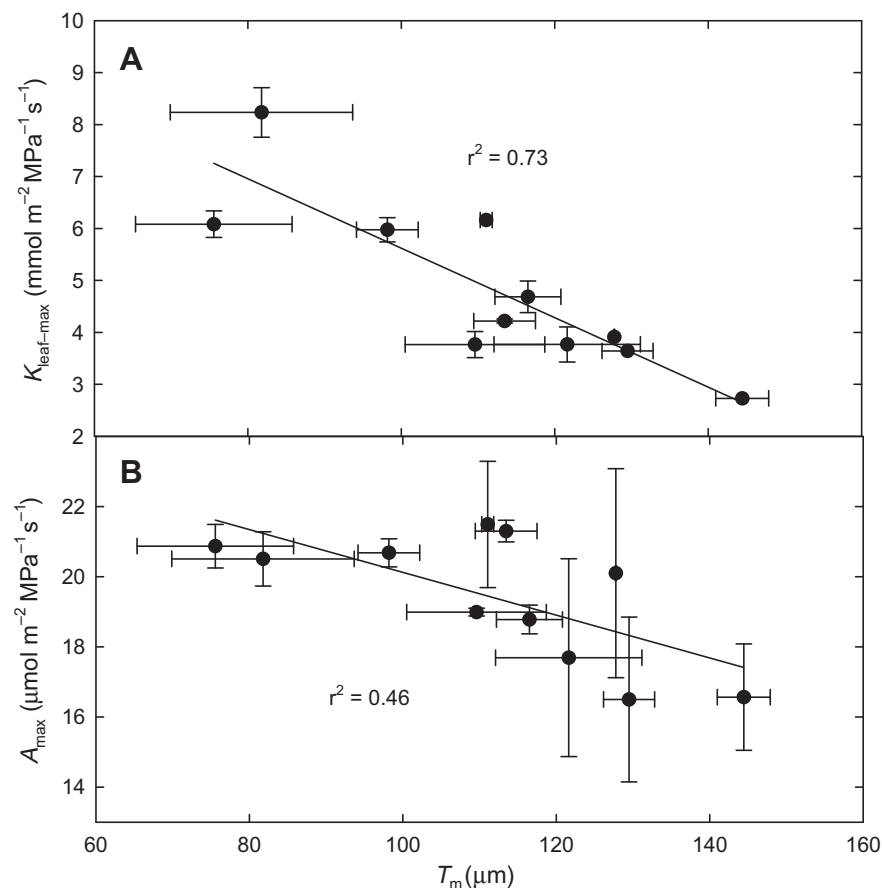


Figure 5. Maximum leaf hydraulic conductance ( $K_{\text{leaf-max}}$ ) versus mesophyll thickness ( $T_m$ ) (A) and maximum photosynthetic rate ( $A_{\text{max}}$ ) versus  $T_m$  (B) in *P. menziesii*. Horizontal bars denote  $\pm$  SE,  $n = 3$  branches for  $T_m$  (A and B). Vertical bars denote  $\pm$  SE,  $n = 2$ –8 branches for  $K_{\text{leaf-max}}$  (A), and  $n = 2$  branches for  $A_{\text{max}}$  (B). Three values in (A) represent trees with only one branch with a  $K_{\text{leaf-max}}$  value and hence lack vertical bars.

$A_{\text{amb}}$  ( $P < 0.0001$ ) highlight their respective roles at different  $\text{CO}_2$  concentrations, and in particular the influence of  $g_m$  on  $A$  at  $C_i$  values that correspond to natural ambient  $[\text{CO}_2]$ . Because our study involved sampling at four distinct stands, there exists the possibility that stand history and factors such as the former or current presence or absence of nitrogen-fixing plants such as *Alnus* spp. may confound analyses of nitrogen variation with height. Nevertheless, the lack of a more significant height-related decline in  $N_A$ , despite the highly significant height-related decline in  $A_{\text{amb}}$  ( $P = 0.00051$ ) suggests a reduction in photosynthetic N-use efficiency with increasing height. Given that thicker needles are less likely to be able to maximize N use on an area basis, the observed height-related trend in N-use efficiency may to some extent be related to the observed height-related patterns in needle anatomy.

The contrast between the strong increase in  $A/g_{\text{s-integrated}}$  and the slight decrease in  $A/g_{\text{s}}$  with increasing height (Figure 4) highlights the role of stomatal control of water loss and the resulting diffusional limitations on photosynthesis in attached shoots. The significant trend in  $A/g_{\text{s-integrated}}$  with height (Figure 4A) is consistent with height-related trends in foliar  $\delta^{13}\text{C}$  or isotope discrimination ( $\Delta$ ) obtained by others (Yoder et al. 1994, McDowell et al. 2002, Koch et al. 2004, McDowell et al. 2005). This height-related increase in intrinsic water-use efficiency is a key component

of the hydraulic limitation hypothesis (Ryan and Yoder 1997). The lack of a height-related increase in  $A/g_{\text{s}}$  for shoots that were sampled along a height gradient, but which had their cut bases in water during the photosynthetic measurements, provides further evidence that path length and gravity are responsible for the height-related trend in  $A/g_{\text{s-integrated}}$ . The slight decline in  $A/g_{\text{s}}$  with increasing height for the cut shoots may reflect a height-related trend in concentrations of osmotic solutes in stomatal guard cells and other leaf cells. Osmotic adjustment that partially maintains leaf cell turgor along a height gradient has been observed in conifers (Koch et al. 2004, Woodruff et al. 2004). Stomatal opening is activated and maintained by a solute-mediated influx of water into the guard cells. Thus, when the impacts of gravity and path length on xylem tension are removed in detached shoots, they may exhibit greater  $g_{\text{s}}$  as a result of the height-related gradient in osmotic concentration.

Estimates of height-related variation of  $A$  in situ ( $A_{\text{integrated}}$ ; Figure 6A) obtained from foliar  $\delta^{13}\text{C}$  values and  $A-C_i$  curves followed a pattern similar to that of  $A_{\text{amb}}$  (Figure 3), although  $A_{\text{integrated}}$  declined more steeply than  $A_{\text{amb}}$  with increasing height. The reductions in mean  $A_{\text{integrated}}$  and  $A_{\text{amb}}$  from the 5 to 55 m sampling heights were 5.64 and 4.03  $\mu\text{mol m}^{-2} \text{s}^{-1}$ , respectively. Integrated  $\text{CO}_2$  assimilation incorporates the stomatal component of

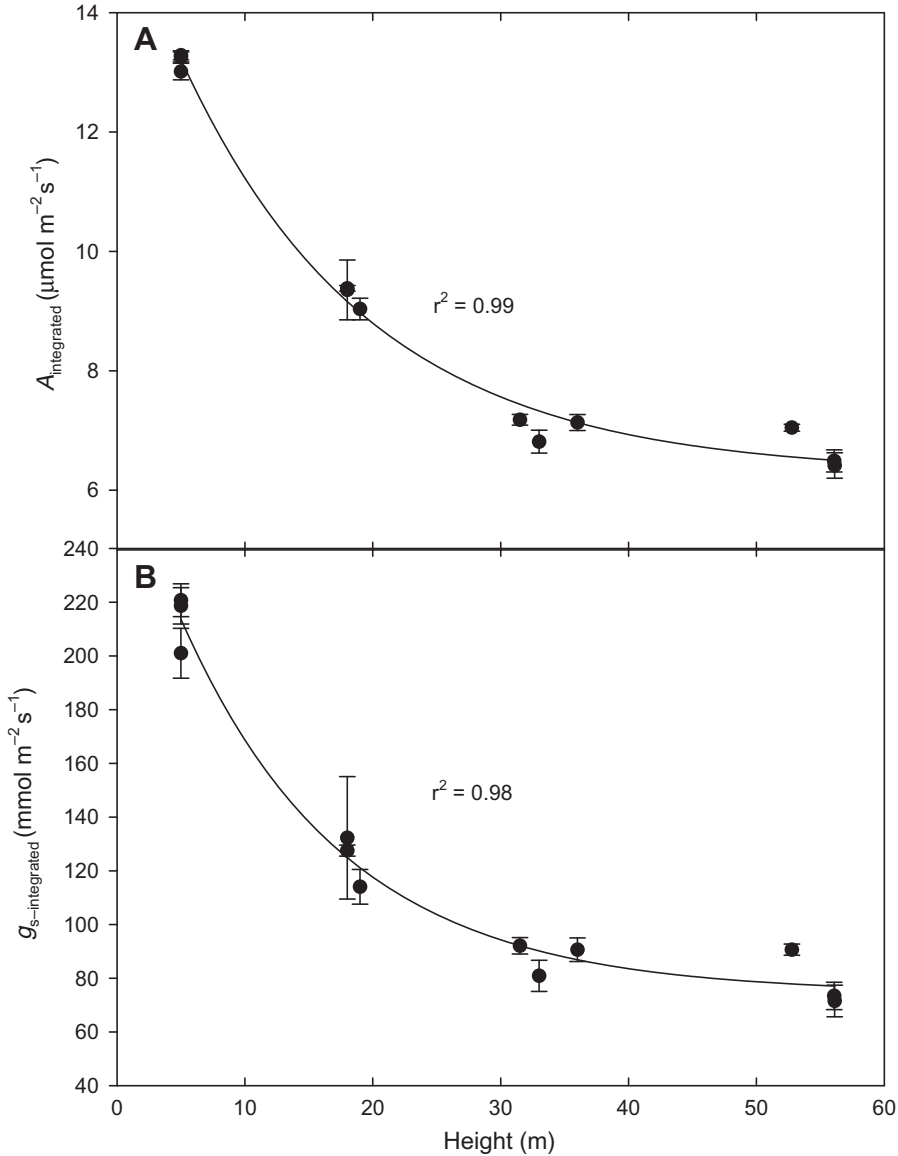


Figure 6. Integrated CO<sub>2</sub> assimilation ( $A_{\text{integrated}}$ ) versus height (A) and integrated stomatal conductance ( $g_{s\text{-integrated}}$ ) versus height (B) in *P. menziesii*. Bars denote  $\pm$ SE,  $n = 3$  branches.

limitation to  $A$  because it represents an estimate of integrated, in situ  $A$ , whereas  $A_{\text{amb}}$  excludes the stomatal component because it is derived from the dependence of  $A$  on substomatal [CO<sub>2</sub>]. Mean integrated values of  $g_s$  ( $g_{s\text{-integrated}}$ ) from the 5 to 55 m sampling heights declined by 2.5 mmol m<sup>-2</sup> s<sup>-1</sup> for every 1 m increase in height (Figure 6B). Although absolute values may not be directly comparable because of the uncertainties associated with estimating stomatal conductance from foliar  $\delta^{13}\text{C}$ , the height-related trends in  $g_m$  and  $g_{s\text{-integrated}}$  suggest that  $g_s$  decreases more rapidly than  $g_m$  with increasing tree height.

Our data support the hypothesis that height-related trends in leaf structure impose constraints on leaf gas exchange that are independent of the direct effects of vertical gradients in xylem tension on stomatal and photosynthetic physiology. Nevertheless, gravity and path length, through their effects on xylem tension during leaf expansion, were likely to have been the principle determinants

of the trends in foliar characteristics that were correlated with the observed height-related trends in gas exchange.

#### Acknowledgments

This work was supported by the USDA Forest Service, Pacific Northwest Research Station Ecosystem Processes Program. The authors thank Ken Bible, Mark Creighton, Matt Schroeder and the rest of the staff at the Wind River Canopy Crane Research Facility located within the Wind River Experimental Forest, T.T. Munger Research Natural Area. The authors also thank Renee Brooks for advice and suggestions pertaining to stable isotope analyses and Peter Beedlow for help with tree climbing and sample collection.

#### References

Aasamaa, K., A. Sober and M. Rahi. 2001. Leaf anatomical characteristics associated with shoot hydraulic conductance,

- stomatal conductance and stomatal sensitivity to changes of leaf water status in temperate deciduous trees. *Aust. J. Plant Physiol.* 28:765–774.
- Abramoff, M.D., P.J. Magelhaes and S.J. Ram. 2004. Image processing with imageJ. *Biophotonics Int.* 11:36–42.
- Abrams, M.D. 1994. Genotypic and phenotypic variation as stress adaptations in temperate tree species: a review of several case studies. *Tree Physiol.* 14:833–842.
- Apple, M., K. Tiekotter, M. Snow, J. Young, A. Soeldner, D. Phillips, D. Tingey and B. Bond. 2002. Needle anatomy changes with increasing tree age in Douglas-fir. *Tree Physiol.* 22:129–136.
- Bauerle, W.L., T.M. Hinckley, J. Cermak, J. Kucera and K. Bible. 1999. The canopy water relations of old-growth Douglas-fir trees. *Trees* 13:211–217.
- Beerling, D.J. and W.G. Chaloner. 1993. The impact of atmospheric CO<sub>2</sub> and temperature change on stomatal density: observations from *Quercus robur* lamas leaves. *Ann. Bot.* 71:231–235.
- Bond, B.J., N.M. Czarnomsky, C. Cooper, M.E. Day and M.S. Greenwood. 2007. Developmental decline in height growth in Douglas-fir. *Tree Physiol.* 17:441–453.
- Boyer, J.S. 1968. Relationship of water potential to growth of leaves. *Plant Physiol.* 43:1056–1062.
- Boyer, J.S., A.J. Cavelieri and E.D. Schulze. 1985. Control of the rate of cell enlargement: excision, wall relaxation and growth-induced water potentials. *Planta* 163:527–543.
- Brodribb, T.J. and M. Holbrook. 2003. Stomatal closure during leaf dehydration, correlation with other leaf physiological traits. *Plant Physiol.* 132:2166–2173.
- Brodribb, T.J., T.S. Field and G.J. Jordan. 2007. Leaf maximum photosynthetic rate and venation are linked by hydraulics. *Plant Physiol.* 144:1890–1898.
- Caird, M.A., J.H. Richards and L.A. Donovan. 2007. Nighttime stomatal conductance and transpiration in C3 and C4 plants. *Plant Physiol.* 143:4–10.
- Carder, A.C. 1995. Forest giants of the world past and present. Fitzhenry and Whiteside, Markham, Ontario.
- DeLucia, E.H., D. Whitehead and M.J. Clearwater. 2003. The relative limitation of photosynthesis by mesophyll conductance in co-occurring species in a temperate rainforest dominated by the conifer *Dacrydium cupressinum*. *Funct. Plant Biol.* 30:1197–1204.
- England, J.R. and P.M. Attiwill. 2006. Changes in leaf morphology and anatomy with tree age and height in the broadleaved evergreen species, *Eucalyptus regnans* F. Muell. *Trees* 20:79–90.
- Ethier, G.J. and N.J. Livingston. 2004. On the need to incorporate sensitivity to CO<sub>2</sub> transfer conductance into the Farquhar–von Caemmerer–Berry leaf photosynthesis model. *Plant Cell Environ.* 27:137–153.
- Farquhar, G.D., S. von Caemmerer and J.A. Berry. 1980. A biochemical model of photosynthetic CO<sub>2</sub> assimilation in leaves of C3 species. *Planta* 149:78–90.
- Farquhar, G.D., M.H. O’Leary and J.A. Berry. 1982. On the relationship between carbon isotope discrimination and the intercellular carbon dioxide concentration in leaves. *Aust. J. Plant Physiol.* 9:121–37.
- Flexas, J., M. Ribas-Carboi, A. Diaz-Espejo, J. Galmes and H. Medrano. 2008. Mesophyll conductance to CO<sub>2</sub>: current knowledge and future prospects. *Plant Cell Environ.* 31: 602–621.
- Givnish, T.J. 1988. Adaptation to sun and shade: a whole plant perspective. *Aust. J. Plant Physiol.* 15:63–92.
- Gould, G.W. and J.C. Measures. 1977. Water relations in single cells. *Philos. Trans. R. Soc. Lond. B* 278:151–166.
- Gower, S.T., R.E. McMurtrie and D. Murty. 1996. Above-ground net primary production decline with stand age: potential causes. *Trends Ecol. Evol. Res.* 11:378–382.
- Gutschick, V.P. 1999. Biotic and abiotic consequences of differences in leaf structure. *New Phytol.* 143:3–18.
- Haffner, V., F. Enjalric, L. Lardet and M.P. Carron. 1991. Maturation of woody plants: a review of metabolic and genomic aspects. *Ann. For. Sci.* 48:615–630.
- Hanba, Y.T., S.-I. Miyazawa and I. Terashima. 1999. The influence of leaf thickness on the CO<sub>2</sub> transfer conductance and leaf stable carbon isotope ratio for some evergreen tree species in Japanese warm-temperate forests. *Funct. Ecol.* 13:632–639.
- Hsiao, T.C., E. Acevedo, E. Fereres and D.W. Henderson. 1976. Stress metabolism: water stress, growth and osmotic adjustment. *Philos. Trans. R. Soc. Lond. B* 273:479–500.
- Kirkham, M.B., W.R. Gardner and G.C. Gerloff. 1972. Regulation of cell division and cell enlargement by turgor pressure. *Plant Physiol.* 49:961–962.
- Koch, G.W., S.C. Sillett, G.M. Jennings and S.D. Davis. 2004. The limits to tree height. *Nature* 428:851–854.
- Loreto, F., S. Delfine and A. Alvino. 1997. On the contribution of mesophyll resistance to CO<sub>2</sub> diffusion to photosynthesis limitation during water and salt stress. *Acta Hort.* 449:417–422.
- McDowell, N.G., N. Phillips, C.K. Lurch, B.J. Bond and M.G. Ryan. 2002. An investigation of hydraulic limitation and compensation in large, old Douglas-fir trees. *Tree Physiol.* 22:763–774.
- McDowell, N.G., J. Licata and B.J. Bond. 2005. Environmental sensitivity of gas exchange in different-sized trees. *Oecologia* 145:9–20.
- Meinzer, F.C., J. Warren and J.R. Brooks. 2007. Species-specific partitioning of soil water resources in an old-growth Douglas-fir–western hemlock forest. *Tree Physiol.* 27:871–880.
- Mencuccini, M. and J. Grace. 1996. Developmental patterns of above-ground hydraulic conductance in a Scots pine (*Pinus sylvestris* L.) age sequence. *Plant Cell Environ.* 19:939–948.
- Mencuccini, M., J. Martinez-Vilalta, H.A. Hamid, E. Korakaki and D. Vanderklein. 2007. Evidence for age- and size-mediated controls of tree growth from grafting studies. *Tree Physiol.* 27:463–473.
- Niinemets, Ü. 1997. Distribution patterns of foliar carbon and nitrogen as affected by tree dimensions and relative light conditions in the canopy of *Picea abies*. *Trees* 11:144–154.
- Niinemets, Ü. 2002. Stomatal conductance alone does not explain the decline in foliar photosynthetic rates with increasing tree age and size in *Picea abies* and *Pinus sylvestris*. *Tree Physiol.* 22:515–535.
- Niinemets, Ü., C. Alessandro, M. Rodeghiero and T. Tosens. 2005. Leaf internal diffusion conductance limits photosynthesis more strongly in older leaves of Mediterranean evergreen broad-leaved species. *Plant Cell Environ.* 28:1552–1566.
- Osborn, J.M. and T.N. Taylor. 1990. Morphological and ultrastructure studies of plant cuticular membranes. I. Sun and shade leaves of *Quercus velutina* (Fagaceae). *Bot. Gaz.* 151:465–476.
- O’Toole, J.C., R.K. Crookston, K.J. Treharne and J.L. Ozbun. 1976. Mesophyll resistance and carboxylase activity, a

- comparison under water stress conditions. *Plant Physiol.* 57:465–468.
- Parkhurst, D.F. 1986. Internal leaf structure: a three-dimensional perspective. *In* On the Economy of Plant Form and Function. Ed. T.J. Givnish. Cambridge University Press, Cambridge, pp 215–249.
- Peña-Rojas, K., X. Aranda, R. Joffre and I. Fleck. 2005. Leaf morphology, photochemistry and water status changes in resprouting *Quercus ilex* during drought. *Funct. Plant Biol.* 32:117–130.
- Ryan, M.G. and B.J. Yoder. 1997. Hydraulic limits to tree height and tree growth. *Bioscience* 47:235–242.
- Sharkey, T.D., C.J. Bernacchi, G.D. Farquhar and E.L. Singsaas. 2007. Fitting photosynthetic carbon dioxide response curves for C3 leaves. *Plant Cell Environ.* 30:1035–1040.
- Shaw, D.C., J.F. Franklin, K. Bible, J. Klopatek, E. Freeman, S. Greene and G.G. Parker. 2004. Ecological setting of the wind river old-growth forest. *Ecosystems* 7:427–439.
- Syvrtsen, J.P., J. Lloyd, C. McConchie, P.E. Kriedemann and G.D. Farquhar. 1995. On the relationship between leaf anatomy and CO<sub>2</sub> diffusion through the mesophyll of hypostomatous leaves. *Plant Cell Environ.* 18:149–157.
- Warren, C.R. 2008. Stand aside stomata, another actor deserves centre stage: the forgotten role of the internal conductance to CO<sub>2</sub> transfer. *J. Exp. Bot.* 59:1475–1487.
- Warren, C.R., G.J. Ethier, N.J. Livingston, N.J. Grant, D.H. Turpin, D.L. Harrison and T.A. Black. 2003. Transfer conductance in second growth Douglas-fir (*Pseudotsuga menziesii* (Mirb.) Franco) canopies. *Plant Cell Environ.* 26:1215–1227.
- Warren, C.R., N.J. Livingston and D.H. Turpin. 2004. Water stress decreases transfer conductance of Douglas-fir (*Pseudotsuga menziesii* (Mirb.) Franco) seedlings. *Tree Physiol.* 24:971–979.
- Warren, J.M., F.C. Meinzer, J.R. Brooks and J.C. Domec. 2005. Vertical stratification of soil water storage and release dynamics in Pacific Northwest coniferous forests. *Agric. For. Meteorol.* 130:39–58.
- Woodruff, D.R., B.J. Bond and F.C. Meinzer. 2004. Does turgor limit growth in tall trees? *Plant Cell Environ.* 27:229–236.
- Woodruff, D.R., F.C. Meinzer and B. Lachenbruch. 2008. Height related trends in leaf xylem anatomy and hydraulic characteristics in a tall conifer: safety versus efficiency in foliar water transport. *New Phytol.* 180:90–99.
- Yoder, B., M.G. Ryan, R.H. Waring, A.W. Schoettle and M.R. Kaufmann. 1994. Evidence of reduced photosynthetic rates in old trees. *For. Sci.* 40:513–527.